VISUAL MICROSCOPIC INVESTIGATIONS ABOUT THE ROLE OF pH, SALINITY AND CLAY ON OIL ADHESION AND RECOVERY

Igor Bondino[1], Shashvat Doorwar[2], Raed Ellouz[3], Gerald Hamon[1]
[1] Total E&P, Pau, France; [2] The University of Texas at Austin; [3] ESPCI, Paris, France

This paper was prepared for presentation at the International Symposium of the Society of Core Analysts held in Napa Valley, California, USA, 16-19 September, 2013

ABSTRACT

Low salinity waterflooding has been a subject of great interest in the past decade. Although it has been shown at various scales of investigation and with various means that salinity changes in the injected water can be responsible for increased oil recovery, it must be noted that negative responses have also been reported in the literature and that in any case the predictability of the magnitude of the effect for a given field or rock sample remains very limited. A model that is able to explain this diversity of behaviors and most notably point out the reasons why the process works in some conditions but not in others is still missing. In this work several simple laboratory tests were designed and carried out to investigate the role of salinity, clay, pH on the initial wettability and recovery during a low salinity waterflood. The first type of tests focused on the development of a simple procedure which used glass test tubes and sands as the rock surrogate to study the development of rock/water/oil interactions for rapid screening of suitable pH, with the idea in mind that for every different combination of a rock/oil/brine system there will exist a different pH window for which one would expect to see a low salinity effect. The idea was extended to study the effect of clay on oil adhesion to sand and the nature of emulsions formed during the process. To make our investigation more relevant to the type of dynamic flow conditions expected in porous media, the study continued using glass micromodels where oil recovery experiments were carried out in both secondary and tertiary conditions. In this part of the work, a key element was represented by the development of a new experimental technique for clay (kaolinite) deposition and stabilization inside a glass micromodel which has allowed, for the first time to our knowledge, to produce a synthetic clay-coated transparent porous medium to run low salinity waterflooding experiments at reservoir rates. Our investigations showed that oil adhesion to silica is altered by both salinity and pH gradient and most importantly that not all sands show the same response. Kaolinite appeared to have a major role in all types of experiments with a clear tendency to produce more water wetting systems. A number of microscopic low salinity effects were evident in the micromodel experiments, although oil recovery was overall not enhanced.

INTRODUCTION

Waterfloods have been performed in oil fields for decades as a primary mechanism for secondary oil recovery. During waterflooding, water, usually reservoir formation brine or

sea brine is injected into the formation through the injector wells while maintaining the reservoir pressure to push the oil into the producer well. Poor sweep efficiency and low oil recovery remain the main drawbacks of waterflooding and despite many attempts at improving its production efficiency by employing chemical EOR and gas injection, this relatively simple and inexpensive technique still remains the most widely applied oil recovery technique even today. Historically, the salinity of injection brine was never considered to be a key factor in influencing the efficiency of a water flood. Preferentially it was chosen to be close to the reservoir formation brine concentration to avoid risks of formation damage. However, in the past couple of decades numerous researchers in laboratories around the world ([1, 2, 3, 4, 5]) and some field pilots in single well and inter-well scale field trials ([6, 7, 8, 9, 10, 11]) have indicated that the injection brine salinity can substantially influence oil recovery through waterflooding. The possibility of improving waterflood recoveries through selection of the injection water, or changing the composition of the injection water during later stages of the flood, has obvious practical benefits. Despite extensive research, however, the involved mechanisms of low salinity effects are not clearly identified as of yet due to the complexity of oil/brine/rock interactions. The general consensus among researchers is that injecting low salinity brine somehow creates a wetting state of the rock more favorable to oil recovery. Given the various conditions under which low salinity water injection may or may not lead to additional recovery and the conflict between the conditions under which low salinity injection has proved beneficial in some core floods and failed in others, it is likely that the observed additional recovery in low salinity flood is a net product of more than one mechanism, one dominating over others under a certain condition or all failing together in another condition: therefore the objective of this work is to perform visual investigations in much less complex/heterogeneous systems than what encountered in cores (or reservoirs), similarly to what done by [12, 13], to possibly observe mechanisms that can be linked to improved recovery by low salinity injection.

DESCRIPTION OF EXPERIMENTAL PROCEDURES

Brines and oil

Two brines are used in this study: a high salinity brine (HS: 45 g/l NaCl + 11.8 g/l CaCl2) and a low salinity brine (LS: 1 g/l NaCl). The crude oil has the following properties: TAN 0.31 mg/g KOH; TBN 1.85 mg/g KOH; Density at 20°C/50°C: 866/844 Kg/m3; Viscosity at 20°C/50°C: 26/6 cP; asphaltene content: 5 %.

Oil adhesion tests with sands

These simple laboratory tests are used for rapid screening of a suitable pH window for the rock/water/brine system under study as it has been pointed out by [14] that for every different combination of a rock/oil/brine system there is a specific pH window for which one would expect to see a low salinity effect. To perform the experiments, high salinity (HS) and low salinity (LS) brine samples were prepared at the desired values of pH ranging between acidic pH of 4 to basic pH of 8.5. Clean silica sand from Fontainebleau and Landes were used in the study. The sand was first washed with an acid solution to eliminate all contamination by iron and then neutralized with sodium bicarbonate

followed by washing with distilled water and drying. Clean glass test tubes were filled with HS brine at allotted pH, sealed and left in a thermostatic chamber at 50°C for 48 hours to allow for equilibration with the glass surface. The HS brine was then discarded and equal amount of sand was put in each test tube followed by the HS brine of the same pH as before. The tubes were again left to equilibrate for 2 days at 50°C. During this equilibrium time the pH was constantly monitored and adjusted if required. It was observed that Fountainebleu sand tends to show a buffering nature. After 2 days of aging, excess water was drained from the tubes and the rest soaked into a dry tissue. The wet moist sand was then left again in the thermostatic chamber for 2 hours and then identical amount of oil was added into each tube (approximately 30% of the sand volume) and mixed. The system was then left to equilibrate for 2 days in a thermostatic chamber stirring twice per day. After the aging with oil, each test tube was filled with either HS brine or LS brine (depending on the test) at the chosen pH (Table 2). The thickness of the segregated layer was immediately measured and a record of this thickness was kept for the next two days. On the last day, the tubes are shaken to free the oil that is trapped under to the weight of the sand and not actually adhering to the sand. This helps to correctly estimate the actual sand and oil adhesion. Experiments were repeated twice: overall, reproducibility was observed with only minor variations.

Oil adhesion/emulsion tests without sands

These experiments were also conducted in a thermostatic chamber at 50°C and with clean glass vials. The vials were filled with brine, aged and then a fixed amount of oil was poured into each vial. After oil and brine has equilibrated for one day each tube was vigorously shook for about 3 seconds to force an emulsion: the emulsion was then allowed to separate into two phases. The oil-water segregation was carefully recorded.

Glass micromodel experiments

Micromodels, although simplified representations of naturally occurring rocks, can be beneficial in the study of the low salinity mechanism because they can offer the possibility to observe the pore level mechanisms occurring during a low salinity flood. In these experiments an injection protocol was used which limited the inlet dead volume to around 6 µl, thus avoiding that brines with different salinities have the time to exchange before entering the porous pattern (a concern given the small injection rates used in this study, i.e. 0.1 PV/hr). Two different types of micromodels were used; Table 1 presents the specifications of the micromodels and relative nomenclature (1D, 2D).

Clay coating (kaolinite) of micromodel pores

The motivation for "clay coating" micromodels is that kaolinite and similar clays are probably a major determinant in the low salinity water flooding oil recovery mechanism [15]. Therefore, the first step was to prepare a suspension of kaolinite suitable for injection into the micromodel. This suspension must be sufficiently concentrated to be able to deposit enough kaolinite in the micromodel while having fine particles of kaolinite. We were inspired by the work of [16] to set up this procedure. Well crystallized kaolinite KGa-1b (Washington County, Georgia; clay Minerals Society Source Clay

Repository) was used without further cleaning. The concentration of the resulting dilute suspension of Kaolinite is 0.31 wt% which resulted optimal for injection in the micromodel avoiding pore plugging. Once the suspension was ready, a procedure had to be devised for the actual clay coating of the pore walls: this required several tests before an optimized and successful protocol could be established. In practice, both the amounts of suspension injected and the injection rates had to be adjusted to obtain a quasi-homogeneous distribution in the porous network. For the 1D micromodels, this consisted of injecting four times 0.2 ml of the suspension at different flow rates from 3 ml/hr to 0.5 ml/hr. The conclusive steps are represented by drying in the oven at 80°C for 3 days and then heating with the heating gun at 200°C for 1 min. The temperature of the heatgun had to be raised to 200°C, when compared to the 120°C used by [16], otherwise the deposited clay would flow out of the micromodel with any injected water (whatever its pH and salinity). This higher temperature should not cause any clay degradation (for example transition to dickite, [17]). The result can be appreciated in Figure 1. A necessary comment is that these artificial clay deposits might not be representative of naturally occurring clay.

Table 1. Micromodel characteristics

Micromodel (nomenclature)	Dimension	Pore volume	Channel depth	Pore diameter ranges
1 D 'small pores'	**10 X 60 mm**	**~6 µl**	**25 µm**	**60-200 µm**
2 D Main	**60 X 60 mm**	**~ 100 µl**	**50 µm**	**110-250 µm**

Table 2. Experimental protocol for test tube experiments

		Tube1	Tube 2	Tube3	Tube4	Tube5
Protocol 1	Initial	HS, pH 4	HS, pH 5	HS, pH 6	HS, pH 7	HS, pH 8.5
	Final	HS, pH 4	HS, pH 5	HS, pH 6	HS, pH 7	HS, pH 8.5
Protocol 2	Initial	HS, pH 4	HS, pH 5	HS, pH 6	HS, pH 7	HS, pH 8.5
	Final	LS, pH 4	LS, pH 5	LS, pH 6	LS, pH 7	LS, pH 8.5

OIL ADHESION TESTS WITH SANDS

The first experiment used protocol 1: 5 test tubes at pH of 4, 5, 6, 7 and 8.5 were prepared. HS brine was added in the end to study the effect of only pH on wettability state of silica sand: in this experiment there is therefore no use of low salinity brine. Figure 2 shows the test tubes at the end of the experiment whilst Figure 3 shows a higher resolution details of the same test for the tubes at pH=4, 6, 8.5. A much better adhesion of oil to sand at acidic pH (in line with [16]) is visible: the amount of oil "produced" is also far lower as this tube shows the least amount of oil floating up to the water surface. We noted that oil adhesion increases drastically below pH=5. Figure 4 shows the equivalent test but adding LS brine as a "flooding brine" (protocol 2): as observed before, the most oil wet conditions were again observed in the most acidic pH range, with most oil being retained by the sand (very little amount of oil appears to be floating). Nevertheless it is interesting to note that at higher pH, the sand appears now whitish, with more oil floating

up to the surface than in Figure 3 (for equivalent pH): this could be attributed to a LS effect. Obviously such LS effect does not appear at pH=4, possibly indicating that LS response might be intrinsically linked to the prevalent pH (at least for these tests). A third test (Figure 5) was conducted still using protocol 2, with the following variation: the Fontainebleau sand was beforehand soaked in a suspension of kaolinite and was then left to dry in an oven (at T=60°C) until all water had evaporated. Surprisingly, there was now no oil adhesion to the sand, whatever the pH. It could be argued that either the sand (or the clay coating the sand grains) had been rendered strongly water wet or that the final shaking step of our procedure liberated the clay particles coating the sand together with the oil adhering to it (which could still mean that the sand was water wet). The last test (Figure 6) involved changing the sand: Landes sand and protocol 2 were used. In this case no oil to sand adhesion was observed. To resume: 1) oil adhesion is clearly seen to depend on prevalent pH conditions but the phenomenon appears to be strongly sand dependent; 2) a low salinity effect of oil desorption from the sand was visible (obviously for the sand to which oil could adhere) but the role of pH in the amount of desorption seems decisive; 3) clay-coated sand was seen to neutralize any pH effect and show a behavior which, from a practical point of view, can be associated to enhanced water wetness.

Figure 1. Optical microscope images of clay agggregations in dry micromodel (natural and polarised light).

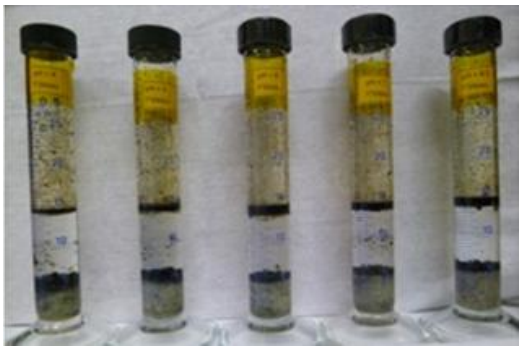

Figure 2. Test tube experiment (protocol 1) with Fontainebleau sand. From left to right: pH=4, 5, 6, 7, 8.5.

Interpretation: Landes Vs Fountainebleu sand

The most striking observation so far is the strong difference in adhesion behaviour between the two sands. As an effort to explain this result, the first consideration came from comparing the shape of Fontainebleau and Landes sand grains, Fontainebleau grains having a higher prevalence of sharp edges, corners and flat faces whilst Landes grains being of bigger dimension, rather well rounded and polished, which might have contributed to its observed non-adhesion nature. Similar observations can be found in the literature [18].

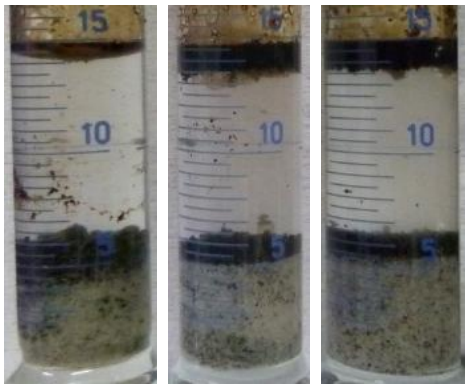

Figure 3. Detail of test tubes at pH=4, 6, 8.5, from left to right. Fontainebleau, protocol 1.

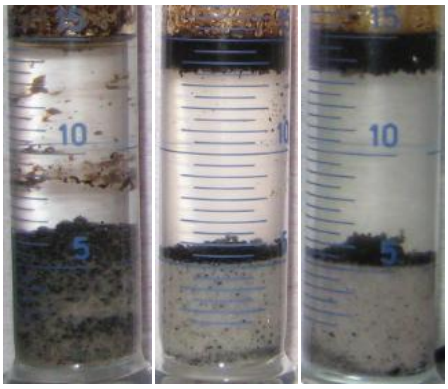

Figure 4. Detail of test tubes at pH=4, 6, 8.5, from left to right. Fontainebleau, protocol 2.

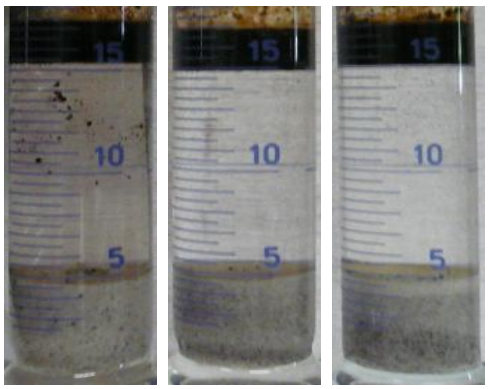

Figure 5. Detail of test tubes at pH=4, 6, 8.5, from left to right. Clay-coated Fontainebleau, protocol 2.

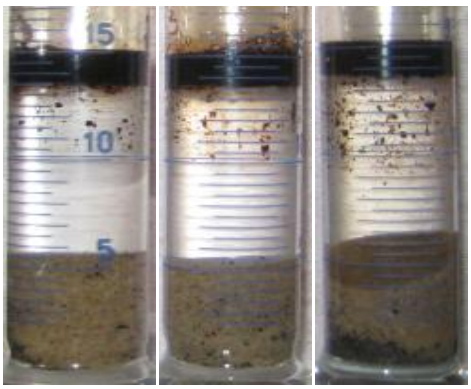

Figure 6. Detail of test tubes at pH=4, 6, 8.5, from left to right. Landes sand, protocol 2.

On the other hand it is also possible to support a different explanation: elementary and mineralogical composition analysis have showed that although the two sands are similar, the only significant difference in elementary composition is the difference in the content of Al_2O_3 (0.0 and 0.87 mass% in Fountainebleu and Landes respectively) , K_2O (0.01 and 0.36 mass% in Fountainebleu and Landes respectively) and Fe_2O_3 (0.02 and 0.10 mass% in Fountainebleu and Landes respectively) whilst, on comparing the mineralogy composition, the only substantial difference relates to the microcline content ($KAlSi_3O_8$; (0.2 and 2.5 mass% in Fountainebleu and Landes respectively). Assuming microcline is chemically inert, we take the suggestion from [19] to propose that a slightly different amount of iron could be responsible for the observed trends. These authors, in their study of wettability alteration in quartz and iron oxide coated sand system, proved that a thin coating of iron oxide over sand can render it strongly water wet. This can be explained on the basis of iso-electric point and pH of the system: at a sufficiently low pH (protonation point), the protons from the medium protonate the organic base (oil in this case), developing a positive charge over it: this may occur at a pH of around 5 for our oil brine system (below this pH a steep increase in oil adhesion is always noticed in the test tube experiments with Fountainebleu sand). Meanwhile, at the isoelectric point of silica (pH 2.5), the net-surface charge of the solid surface transitions from positive to negative:

silica will possess a net negative charge above its isoelectric point and become increasingly negative as pH increases further. Thus, in the range of pH 2.5 to 5, there is an electrostatic attraction between the negative silica surface and positive charge of the protonated oil blob. This also explains the oil wetting trend in the acidic pH range for our experiments with silica sand. [19] also suggest that the presence of an iron oxide layer over silica sand shifts its isoelectric point to around pH 6.5. So the silica sand has a positive surface charge below the pH of 6.5 and being the oil blobs protonated, there is an net electric repulsion between sand and oil which would then explain the results with Landes sand at pH 4, 5 and 6. Above pH 6.5 the sand becomes weakly negative but since the oil is no longer protonated or weakly protonated, attraction (adhesion) is either absent or very weak.

Emulsion/adhesion tests (no sand)

During the experiments with sand, it was observed that the oil that floats up is in a different emulsion state depending on whether the pH was acidic or basic. To verify this observation about emulsions, a complementary test was performed which was also conducted in a thermostatic chamber at 50^{o}C and with clean glass vials. The vials were filled with brine, aged and then a fixed amount of oil was poured into each vial. After oil and brine has equilibrated for one day each tube was vigorously shook for about 3 seconds to force an emulsion; the emulsion was then allowed to separate into two phases. The oil-water segregation was carefully recorded. Figure 7 shows the comparison between each tube and also between the initial and final stages. Comparison of the high salinity tubes show that the oil adhesion or oil wettability increases as the pH decreases. The glass wall in the brine phase of the tube with pH 4 has oil drops sticking all over it. As we move towards the high pH end, oil adhesion is remarkably reduced and the glass surface in aqueous phase looks clearer. This behavior is consistent with our observations on oil adhesion in sand experiments. Comparison with the low salinity also shows a similar trend but in a much moderate manner. There is a very slight adhesion to glass at the acidic pH of the LS brine and, as we move towards the basic pH, there is no visible adhesion to the glass. These results are also consistent with the experiments with sand. It can be concluded that glass and Fontainebleau silica sand have a similar response to salinity and pH. This result is significant because all experiments with micromodels use glass. During the experiment it was observed that both the visual aspect of the emulsions formed in the tubes and their settling rates depended strongly on pH. The emulsions formed in the low salinity system (especially the ones with high pH) took very long to settle down and no discernible oil drops could be seen floating around: the aqueous phase appeared like a homogeneous brown colored phase. The brownish coloration slowly disappeared as the phases separated. Figure 8 shows the snapshots of the recorded videos. The schematic in Figure 9 synthetizes our comprehension for the observed wettability trends on the basis of protonation and iso-electic point of the surface, with two extreme examples, for HS and LS brines.

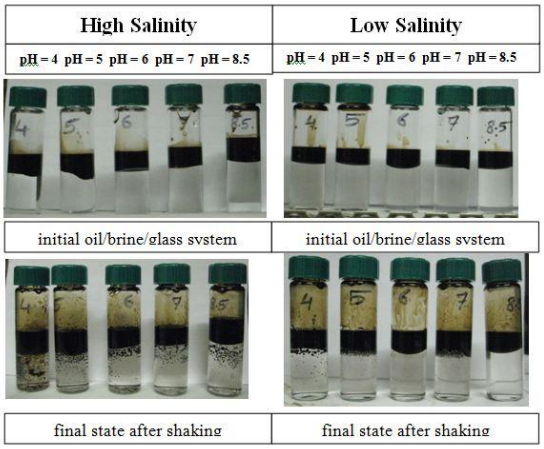

pH 8.5	N	A
pH 7	N	A
pH 6	N/T	A
pH 5	T	A
pH 4	A	A
	LS	HS

Figure 7. Test with glass vials at pH=4,5,6,7,8.5 from left to right. Bottom: corresponding adhesion chart.

Figure 8. Snapshots taken at same time to show the difference in between the settling rates of the emulsions formed for HS and LS brine at t = 20,50,80,100 secs.

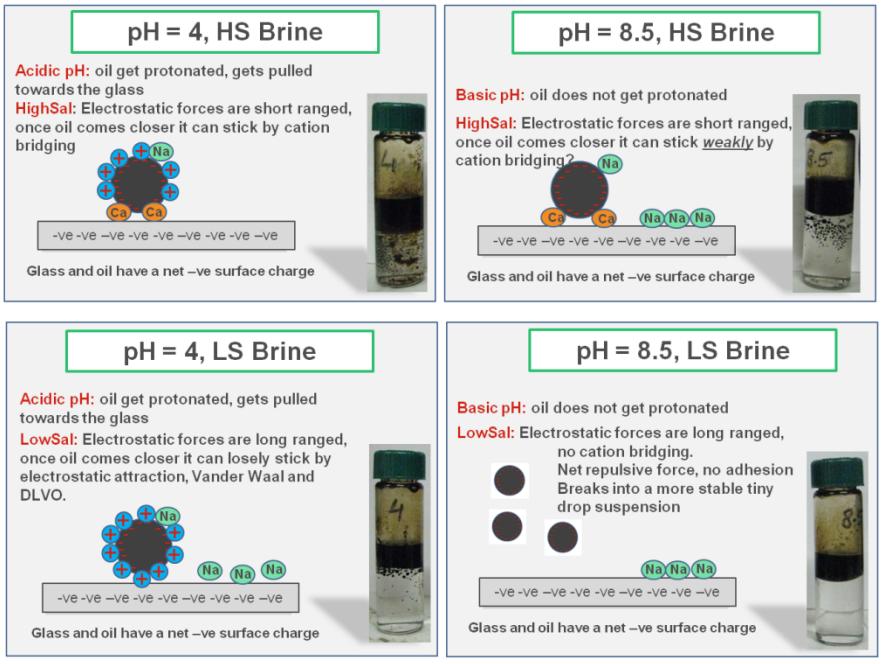

Figure 9. Schematic explanation of the possible mechanism of oil adhesion.

MICROMODEL INVESTIGATIONS

Twelve micromodel experiments were performed at very slow rate (2 PVs injected for a HS flood, 2 to 4 PVs injected for a LS flood, very low flow rates of 0.1PV/hr) varying/combining the following parameters: presence of clay, secondary Vs tertiary floods, salinity (HS and LS), pH (4.5, 7, 8.5), temperature (20°C and 50°C). Initial saturations were established by saturating the system with HS water, then performing oil drainage. We resume here the main results in a synthetic way. Figure 10 highlights the differences encountered when flooding 1D micromodels free of clay (T=20°C, pH=7). Case a correspond to a secondary high salinity flood; b to a secondary low salinity flood; c to secondary high salinity flood in a clay coated micromodel; d to a secondary low salinity flood again with clay. Each of the 4 snapshots represents an image difference between the micromodel at the end of the waterflood and the same micromodel at the beginning of the waterflood: white areas correspond to areas where oil has been produced. We note that in clay-free micromodels (a, b), oil has been displaced from the bulk of the pore being swept by "main terminal menisci" as in a piston-like displacement (a water front was also well discernible in the micromodel during the flood). On the other hand (c, d), when clay is present, no water front was ever seen and oil was displaced purely by thickening of the water layers. These very different pore-scale mechanisms explain the remarkably different appearance between a/b and c/d. These water layers were seen to be very thick: their formation originated during the oil drainage phase, where advancing oil was effectively repulsed by clay (as in an electrostatic repulsion) leaving thick water spaces in between clay and oil. This is observable in the example of Figure 10e. Image analysis performed on these first 4 experiments (experiment N1 – N4) did not lead to any conclusion regarding oil production (because of clay presence/absence or salinity content): this could also have been due to finite size effects or reduced connectivity dominating the displacement.

Experiment N5 (T=20°C, pH=7, clay) was a tertiary LS flood in a 1D micromodel: the micromodel behaved as strongly water wet (after 2 days of aging at room temperature) with oil recovered via water layer thickening during the HS flood. No LS improved recovery was visible. Experiment N6 was run in a 1D micromodel with (T=20°C, pH=4.5, no clay): a switch to acidic pH of the connate and HS brine was inspired from the results of our test tube experiments to render the micromodel more oil wet. Despite the oil wet nature of the micromodel, the tertiary acidic LS flood did not show any difference in the tertiary mode. This is consistent with the test tubes experiments where the tertiary LS brine at acidic pH did not result in any significant change. Experiment N7 was run in a 1D micromodel with (T=20°C, pH=4.5, clay): this experiment was an attempt to render kaolinite oil wet in the presence of an acidic brine. The aging at acidic pH of the connate brine failed to make the micromodel oil wet. The water still invaded through films and the model behaved in a strongly water wet manner. This result is consistent with the observation with the Fontainebleau sand (the idea of a tertiary LS flood was thereby dropped in N7). Experiment N8 and N9 were tertiary LS floods (T=20°C, pH=7, no clay) in large 2D micromodel: N8 was run in a brand-new micromodel with water wet conditions and N9 in mixed wet conditions (obtained by aging the micromodel in oil prior to the commencement of the experiment). Quantitative

oil saturation plots become now more reliable (thanks to the bigger dimension of the model) and are proposed: the recovery plots show enhanced recovery in mixed wet when compared to water wet for the HS flood (Figure 11), but no LS effect in both cases. Visual inspection of several images taken during the LS flood confirmed that oil was not desorbed/remobilized/produced. Nevertheless in N9, wettability alteration phenomena were observed with formation of oil beads in several parts of the micromodel. These phenomena happened during the LS flood: oil beads could form in regions where no oil was visible before and their formation/growth would normally last several hours (with LS still flowing, Figure 12). This should indicate a transition towards water wetness. Experiment N10 was conducted with (T=50°C, pH=4.5 for formation and HS brines, pH=8.5 for LS brine; no clay). The experiment was run at increased temperature as the facility became at some point available. The choice of varying the pH of injected waters was to first trigger adhesion (acidic pH) and then desorption (basic pH), possibly facilitating a LS effect. Figure 13 shows a snapshot of a micromodel region at the end of the tertiary salinity flood: although again this experiment showed no quantifiable low salinity effect on recovered oil, this time a darker phase was observed in oil, similarly to what reported by [20]. Oil beading phenomena (wettability alteration) were here prominent. This experiment was repeated (Experiment N11) using the same protocol of N10 but injecting in tertiary mode a basic HS brine (T=50°C, pH=4.5 for formation and HS brines, pH=8.5 for tertiary HS brine; no clay). Without salinity gradient, in this case neither beading of oil nor formation of the darker phase was observed anywhere in the micromodel. It could be concluded that the pore scale phenomena observed in N10 (dark phase in oil) is related to the salinity change and is perhaps intensified in the presence of a proper pH gradient. It should also be noted that the darker phase was never observed in the previous experiments run at lower temperatures. Experiment N12 was conducted with (T=50°C, pH=4.5 for formation and HS brines, pH=8.5 for tertiary HS brine; clay). Acidic connate brine was injected and the oil aged in it for 5 days at 50°C. Even after the aging at elevated temperature and acidic pH the micromodel remained strongly water wet. Towards the end of low salinity flood, again deposition of the dark phase was observed. No LS positive effect was observed.

CONCLUSIONS

It can be concluded from the series of experiments with sands and (sand-less) glass vials that they show a consistent behaviour. Some major consistencies can be shortlisted as: 1) both systems display an oil wetting behaviour at acidic pH; 2) both the glass and sand system show a preference to water wetness at basic pH and low salinity; 3) oil adhesion to silica is altered by both salinity and pH gradient. Furthermore it was observed that not all sands show the same response: an interpretation was provided which could lead to think that for every different crude oil - brine - rock system there will be a different pH window for which oil adhesion-desorption events can be seen, i.e. for which the low salinity effect becomes effective. It was noted that the shape of the sand grain may also influence adhesion. The presence of kaolinite was seen to render the micromodel glass and sand particles strongly water wet. It was shown how different types of oil in water emulsion are formed for different pH and salinity: it appeared that the lower adhesion at

pH 8.5 to glass in LS brine could be because of the formation of very stable oil in water emulsion with tiny droplets of oil floating in water phase. In these pH conditions the micromodel experiments showed formation of a darker phase, which could then be an emulsion. No evidence of any large scale, quantifiable positive impact of low salinity flood on oil recovery was found during dynamic displacement experiment (micromodel). Oil wetting of clay could be the key to see low salinity effect but such condition could not yet be accomplished experimentally inside a micromodel. On the other hand, some microscopic pore scale effects during low salinity floods were observed.

ACKNOWLEDGMENTS

The authors would like to thank TOTAL for financial and technical assistance throughout the course of this study.

REFERENCES

1. Jadhunandan, P.P. and Morrow, N.R.: "Effect of Wettability on Waterflood Recovery for Crude-Oil/Brine/Rock Systems", SPE 22597, 66th Annual Technical Conference, Dallas, TX, 1991.
2. Yildiz, H.O. and Morrow, N.R.: "Effect of Brine Composition on Recovery of Moutray Crude Oil by Waterflooding", Journal of Petroleum Science and Engineering, Vol.14: 159-168, 1996.
3. Tang, G. and Morrow, N.R.: "Salinity, Temperature, Oil Composition and Oil Recovery by Waterflooding", SPE Reservoir Engineering, Vol.12: 269-276, 1997.
4. Boussour, S., Cissokho, M., Cordier, P., Bertin, H., and Hamon, G.: "Oil Recovery by Low Salinity Brine Injection: Laboratory Results on Outcrop and Reservoir Cores", SPE 124277, 2009.
5. Yousef, A.A., Al-Saleh, S., Al-Kaabi, A. and Al-Jawfi, M.: "laboratory Investigation of Novel Oil Recovery Method for Carbonate Reservoirs", CSUG/SPE 137634, 2010.
6. Webb, K.J., Black, C.J.J., and Al-Jeel, H.: "Low Salinity Oil Recovery- Log-Inject-Log", SPE 89379, 2004.
7. McGuire, P.L., Chatham, J.R., Paskvan, F.K., Sommer, D.M., and Carini, F.H.: "Low Salinity Oil Recovery: An Exciting New EOR Opportunity for Alaska's North Slope", SPE 93903, 2005.
8. Lager, A., Webb, K.J., Collins, I.R., and Richmond, D.M. "LoSalTM Enhanced Oil Recovery: Evidence of Enhanced Oil Recovery at the Reservoir Scale", SPE 113976, 2008.
9. Seccombe, J., Lager, A., Jerauld, G., Jhaveri, B., Buikema, T., Bassler, S., Denis, J., Webb, K., Cockin, A., and Fueg, E.: "Demonstration of Low-Salinity EOR at Interwell Scale, Endicott Field, Alaska", SPE 129692, 2010.
10. Skrettingland, K., Holt, T., Tweheyo, M.T., and Skjevrak, I.: "Snorre Low Salinty Water Injection – Core Flooding Experiment and Single Well Field Pilot", SPE 129877, 2010.
11. Mahani, H., Sorop T. G., Ligthelm, D., Brooks, A.D., Vledder, P., Mozahem, F. and Ali Y.: "Analysis of Field Responses to Low-salinity Waterflooding in Secondary and Tertiary Mode in Syria ", SPE 142960, 2011.
12. Berg, S., Cense, A. W., Jansen, E. and Bakker, K.: "Direct experimental evidence of wettability modification by low salinity", Petrophysics 51 (5), 314-322, 2010.
13. Fogden, A. and Lebedeva, E. V.: "Changes in Wettability State due to Waterflooding", International Symposium of the Society of Core Analysts, Austin, Texas, USA, SCA2011-15, 2011.
14. Austad, T., RezaeiDoust, A. and Puntervold, T. "Chemical Mechanism of Low Salinity Water Flooding in Sandstone Reservoirs", SPE 129767, 2010.
15. Morrow, N. and Buckley, J.: "Improved Oil Recovery by Low-Salinity Waterflooding", Journal of Petroleum Technology 63 (5), SPE 129421, 106-112, 2011.
16. Lebedeva, E.V.; Fogden, A.: "Adhesion of oil to kaolinite in water", Environ. Sci. Technol. 44, 9470-9475, 2010.
17. Wang, H., Li, C. and Peng, Z.: "Characterization and thermal behaviour of kaolin", J. Thermal Anal Calorim, 105:157-160, 2011.
18. Michalski, M. C., Desobry, S. and Hardy, J.: "Adhesion of Edible Oils and Food Emulsions to Rough Surfaces", LWT - Food Science and Technology, Vol. 31, Issue 5, August 1998, Pages 495–502.
19. Molnar, I. L., O'Carrol, D.M. and Gerhard, J. I.: "Impact of surfactant-induced wettability alterations on DNAPL invasion in quartz and iron oxide-coated sand systems", J. Contaminant Hydrology, Vol. 119, 1-12, 2011.
20. Emadi, A. and Sohrabi, M.: "Visual investigation of low salinity waterflooding", presented at the International Symposium of the Society of Core Analysts, Aberdeen, Scotland, UK, 27-30 August, SCA2012-53, 2012.

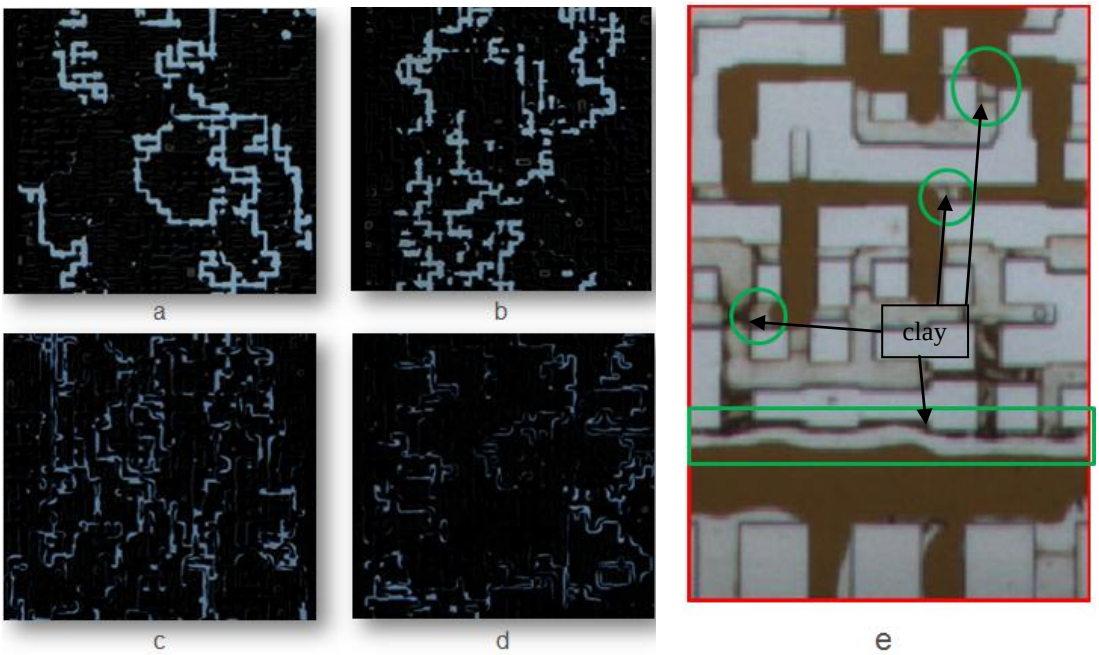

Figure 10. Image differences (end of waterflood minus start of waterflood) for Experiments N1,2,3,4; white is oil recovered (a: HS flood, no clay; b, LS flood, no clay; c: HS flood, clay; d, LS flood, clay). Clay-coated micromodel detail after oil drainage (e): green marks show areas in which thick water layers separate oil from clay.

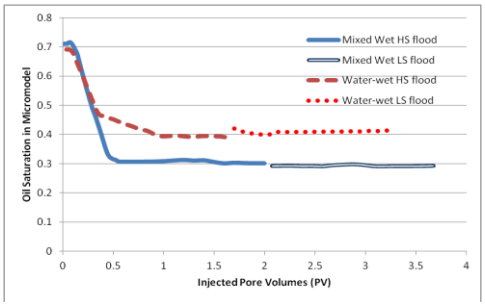

Figure 11. Oil saturation for Experiments 8 (water wet - red) and 9 (mixed wet - blue).

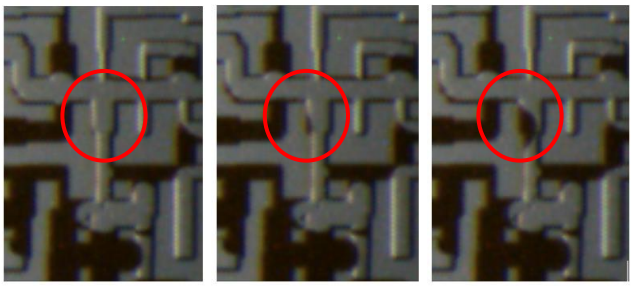

Figure 12. Formation of an oil bead during tertiary LS flood (Experiment N9).

Figure 13. Formation of dark phase in oil during LS flood in Experiment N10.